Ore Geology Reviews 86 (2017) 297–308

Contents lists available at ScienceDirect

Ore Geology Reviews

journal homepage: www.elsevier.com/locate/oregeo

Submarine hydrothermal contribution for the extreme element accumulation during the early Cambrian, South China

Tao Han, Haifeng Fan *, Xiaoqing Zhu, Hanjie Wen, Chenghai Zhao, Fang Xiao

State Key Laboratory of Ore Deposit Geochemistry, Institute of Geochemistry, Chinese Academy of Sciences, Guiyang 550002, China

ARTICLE INFO

Article history:
Received 8 August 2016
Received in revised form 18 February 2017
Accepted 24 February 2017
Available online 27 February 2017

Keywords:
Hydrothermal activity
Coarse-grained limestone
Early Cambrian
South China
Sr isotope
REE

ABSTRACT

Throughout the geological history of the Earth, submarine hydrothermal activity has played an important role in seawater chemistry, biological evolution and enrichment of metals in the Earth crust. However, the prospect of hydrothermal activity for extreme element accumulation during the early Cambrian, a key geological period, in South China has not been well-constrained. This study reports geochemical (e.g. REE and Sr isotope) investigations of a coarse-grained limestone layer and associated calcite veins in Zunyi and Nayong areas, Guizhou Province, to constrain the hydrothermal activity and evaluate the significance of hydrothermal contribution to extreme element accumulation during the early Cambrian, South China. Our results reveal positive Eu anomalies and higher initial $^{87}Sr/^{86}Sr$ ratios (0.7083–0.7150) for carbonate samples than those of early Cambrian seawater, indicating the presence of hydrothermal processes. Combined with constraints from the spatial relationships and coincidence with adjacent mineralization, these hydrothermal processes provide the most probable contribution for polymetallic Ni–Mo–PGE mineralization. Furthermore, there are abundant hydrothermal dolomite and barite-calcite veins in the dolostone of the Dengying Formation, indicating the occurrence of a variety of hydrothermal fluids. Overall, multi-stage hydrothermal pulses with different fluid compositions spanned the Ediacaran–Cambrian transition in South China. In particular, these hydrothermal fluids with positive Eu anomalies and enriched radiogenic Sr, originating from Proterozoic mafic/ultramafic rocks, may have flowed through the underlying Precambrian silicate clastic rocks (e.g., Xiajiang, Banxi and Lengjiaxi Groups) and may have been crucial for the marine environment, biological diversity and extreme element accumulation during the early Cambrian, South China.

1. Introduction

Submarine hydrothermal activity may provide a perspective for understanding the geological processes, geochemical cycling, and the origin and evolution of life throughout the Earth's history (Baross and Hoffman, 1985 and references therein). Hydrothermal activity with hot, volatile-rich hydrothermal solutions may have changed the redox and chemical conditions of seawater, and even resulted in mineralization on and/or below the seafloor (e.g., Baross and Hoffman, 1985; Zierenberg et al., 1998, 2000; Perner et al., 2013). Moreover, the discovery of hydrothermal communities living in hydrothermal venting system also provides a possibility for investigating the origin of early life (e.g. Baross and Hoffman, 1985; Russell and Hall, 1997; Nisbet and Sleep, 2001; Mcdermott et al., 2015 and references therein).

In South China, submarine hydrothermal processes have been suggested to explain extreme element accumulations (e.g., Ni, Mo, Se, PGE, Ba, Si) within the widespread chert (e.g., Li, 1997; Chen et al., 2009; Wang et al., 2012; Fan et al., 2013; Liu et al., 2015), the bedded polymetallic Ni–Mo–PGE mineralization (e.g., Coveney and Chen, 1991; Murowchick et al., 1994; Lott et al., 1999; Li and Gao, 2000; Jiang et al., 2006, 2007) and the super-large barite deposits (e.g., Wang and Li, 1991; Xia et al., 2004; Žák et al., 2003; Pašava et al., 2008; Han et al., 2015a) during the early Cambrian (Fig. 1). However, the hydrothermal contribution for extreme element accumulation has not been well constrained, although marine redox conditions and biological evolution were studied intensively across this crucial Ediacaran–Cambrian transition (e.g., Zhou and Jiang, 2009; Xu et al., 2012a; Pi et al., 2013; Feng et al., 2014; Och et al., 2015; Cai et al., 2015; Wang et al., 2015a; Wen et al., 2015; Cheng et al., 2016; Jin et al., 2016; Zhang et al., 2016). For instance, the polymetallic Ni–Mo–PGE mineralization, has been studied for four decades (Fig. 1), however, entirely different arguments were proposed, such as asteroid

* Corresponding author.
E-mail address: fanhaifeng@mail.gyig.ac.cn (H. Fan).

http://dx.doi.org/10.1016/j.oregeorev.2017.02.030
0169-1368/

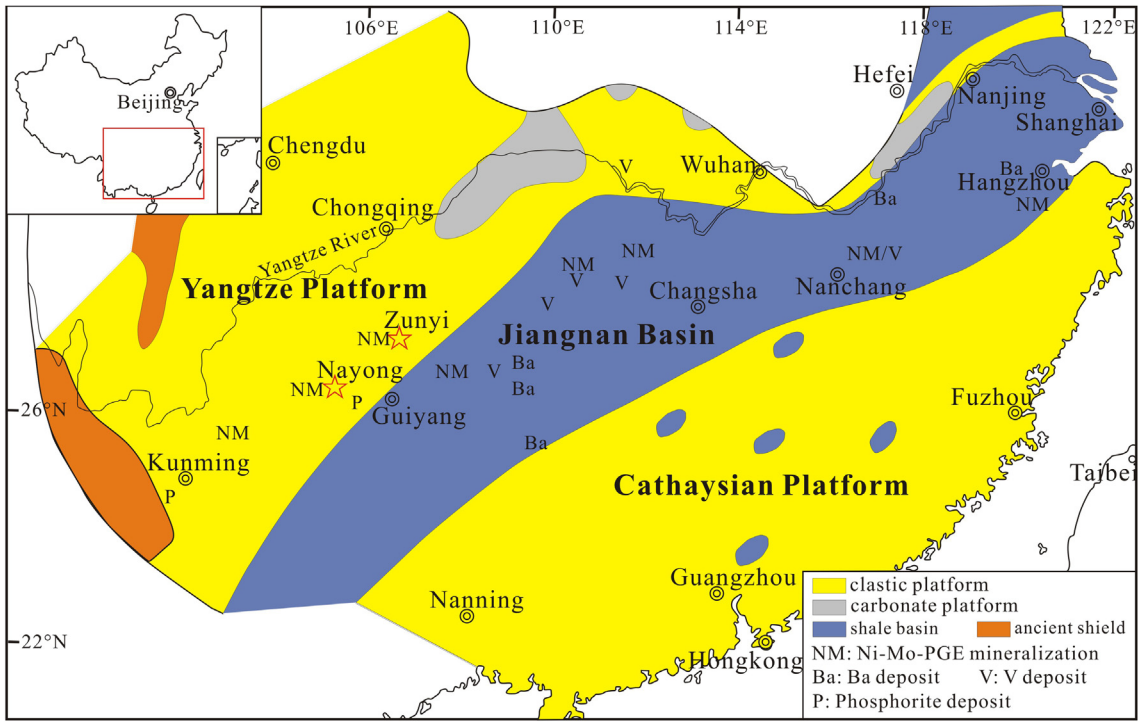

Fig. 1. Lithofacies palaeogeography map and distribution of several mineralization/deposits in the lower Cambrian sedimentary strata along the southern margin of Yangtze Platform (modified from Wang and Li, 1991; Feng et al., 2002; Mao et al., 2002; Coveney and Pašava, 2005; Xu et al., 2014). *Note:* the provincial capitals here represent different provinces.

impact (Fan, 1983), seawater scavenging (Mao et al., 2002; Lehmann et al., 2007, 2016; Xu et al., 2012b), submarine hydrothermal exhalative origin (Coveney and Chen, 1991; Murowchick et al., 1994; Lott et al., 1999; Li and Gao, 2000; Jiang et al., 2006, 2007; Fan et al., 2011; Wen and Carignan, 2011; Cao et al., 2013; Shi et al., 2014; Han et al., 2014; Guo et al., 2016) and multiple sources (Pašava et al., 2008; Han et al., 2015b). Furthermore, it has been proposed that metazoans may have already existed in deep-sea hydrothermal systems during the Precambrian, later migrating from these hydrothermal vents to shallow water in the early Cambrian, according to the mass occurrences of arthropods, sponges and undetermined shells which appear linked to the hydrothermal vents (Steiner et al., 2001). Consequently, hydrothermal activity may have played a crucial role in the extreme enrichment of elements, marine chemical conditions and biological diversity during the early Cambrian, South China.

To constrain the hydrothermal contribution to extreme enrichment of elements during the early Cambrian in South China, a coarse-grained limestone layer closely underlain the polymetallic Ni–Mo–PGE sulfides layer, coupled with nearby geological features across the Ediacaran–Cambrian transition in Zunyi and Nayong areas of Guizhou Province were investigated through the geological, petrographic and geochemical (e.g., REE and Sr isotope) studies. Especially, the characteristics of Eu anomaly and the scope of Sr isotopic signature can effectively identify hydrothermal involvement for extreme metal accumulation.

2. Geological background

The lower Cambrian black shale sequence is well-preserved and widely distributed along the southern margin of Yangtze Platform, which is known as the Niutitang Formation in Guizhou and is equivalent to the Qiongzhusi/Guojiaba Formation in Yunnan and Sichuan, the Muchang/Xiaoyanxi Formation in Hunan, and the Hetang Formation in Zhejiang Province (Fig. 1). The Ediacaran–Cambrian boundary was constrained by SIMS U–Pb zircon ages of 542.1±5.0 Ma and/or 542.6±3.7 Ma in South China where the lower Cambrian black shale is underlain unconformably by the Ediacaran dolostone of the Dengying Formation and/or chert of the Liuchapo Formation (Chen et al., 2015). However, a SHRIMP U–Pb zircon age of 532.3 ± 0.7 Ma from a volcanic ash bed just below the polymetallic Ni–Mo–PGE sulfides layer in the lowermost Niutitang Formation in Zunyi area was also proposed (Jiang et al., 2009).

Several types of significant ore deposits are hosted in these lower Cambrian sedimentary strata of South China (e.g., Emsbo et al., 2005; Xu et al., 2014; Fig. 1). First, the polymetallic Ni–Mo–PGE mineralization, with a few to tens of centimeters thickness, occurs in Yunnan, Guizhou, Hunan, Jiangxi and Zhejiang Provinces contains extremely high Ni, Mo, Zn, TOC (total organic carbon) and total PGE concentrations, which can reach up to 7 wt.%, 8 wt.%, 12 wt.%, 12 wt.% and 943 ppb, respectively (e.g., Xu et al., 2012b; Han et al., 2015b). Second, the phosphorite deposits have been mainly explored in Kunyang of Yunnan and Zhijin of Guizhou. In particular, the Zhijin phosphorite deposit is a uniquely associated REE deposit, with the concentration of total rare earth oxides up to 0.17 wt.% (Jin et al., 2007; Chen et al., 2013). Third, the barium mineralization usually occurs as sediment-hosted stratiform barite deposit, with thicknesses ranging from 3 m to 10 m and content of $BaSO_4$ up to 95 wt.% in Tianzhu of Guizhou, Xinhuang of Hunan, Dongzhi of Anhui and Linan of Zhejiang (Wang and Li, 1991; Fang et al., 2002; Han et al., 2015a). Finally, vanadium deposits are mainly distributed in Tongren of Guizhou, Jishou, Zhangjiajie and Changde of Hunan, Yichang of Hubei and Duchang of Jiangxi. This vanadium-bearing black shale sequence commonly starts from the base of the Niutitang Formation and has a thickness of 7–40 m with the V_2O_5 concentrations of up to 2 wt.% (Hu et al., 2010; Shu et al., 2014).

In Zunyi and Nayong areas of Guizhou Province, South China, the lower Cambrian Niutitang Formation exhibits a similar

variation of lithological stratigraphy from the bottom up as follows (Zeng, 1998; Zhou et al., 2008; Fan et al., 2011; Gao et al., 2011; Han et al., 2015b; and references therein; Fig. 2): (1) A clay layer including a mass of pyrite with a thickness of up to 0.5 m unconformably overlying the dolostone of the Ediacaran Dengying Formation; (2) A phosphate layer with a thickness of up to 1.2 m; (3) A volcanic tuff with a thickness of up to 0.2 m; (4) A bedded chert, usually intercalated with black shale and containing pyrite nodules (0–2 m); (5) The lower black shale with pyrite and apatite nodules (0–8 m); (6) A black coarse-grained limestone layer (0–0.6 m) that cut through vertically by abundant calcite veins; (7) The polymetallic Ni–Mo–PGE sulfides layer with a thickness from 0.02 to 0.6 m, and a maximum thickness of 2 m, which is generally intercalated closely with calcite veins; (8) The upper black shale contains pyrite nodules with a thickness of more than 20 m. However, the volcanic tuff

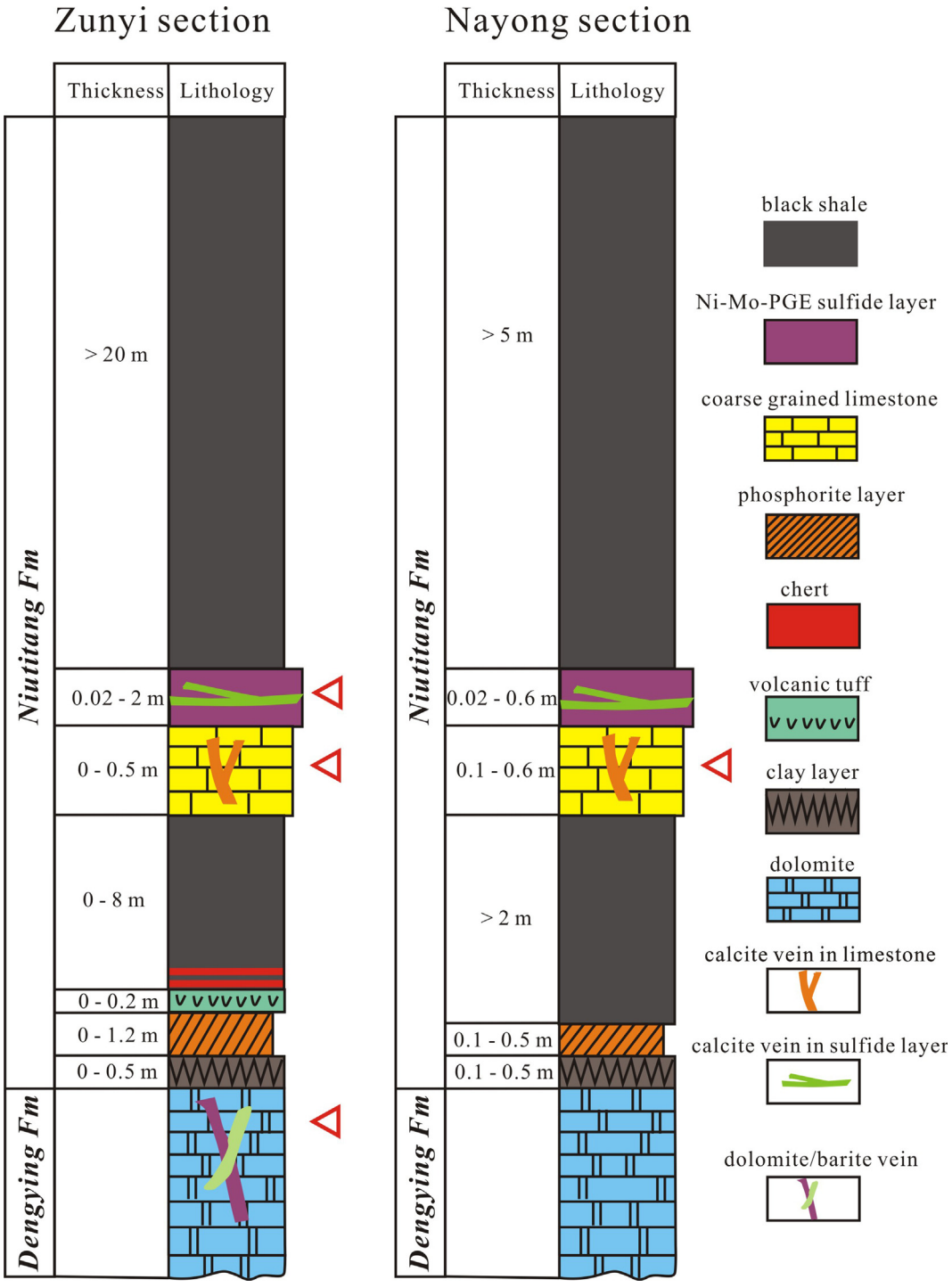

Fig. 2. Integrated lithological stratigraphy of lower Cambrian Niutitang Formation in Zunyi and Nayong areas, Guizhou Province, South China (modified from Zeng, 1998; Zhou et al., 2008; Fan et al., 2011; Gao et al., 2011; Han et al., 2015b; and references therein). The calcite vein that cut through the coarse-grained limestone layer always terminates in the overlain polymetallic sulfides layer. Meanwhile, the other type of calcite veins are commonly closely intercalated within the polymetallic sulfide ores. *Note:* the red triangles represent the stratigraphic position of samples where we collected.

layer reported in Zunyi area has not been found in Nayong area to date (Fig. 2).

3. Materials and methods

The integrated lithological stratigraphy of Niutitang Formation and stratigraphic position of our studied samples in Zunyi and Nayong areas were illustrated in Fig. 2. First, twenty coarse-grained limestone samples were collected from open pits in Zhongnan village of Zunyi County (N 27°41′, E 106°40′) and Shuidong village of Nayong County (N 26°43′, E 105°33′), Guizhou Province. The coarse-grained limestone layer occurs in the form of stratiform (Fig. 3a and b), lenticular (Fig. 3c) and granular structures (Fig. 3d). The typical coarse-grained limestone samples are characterized by gradually decreasing size of calcite grains from bottom to top, which were divided into the lower and upper part in this study (e.g. Fig. 3, Supplementary Materials). In addition, the calcite veins, which cut through vertically the coarse-grained limestone layer but terminated in the overlying polymetallic Ni–Mo–PGE sulfides layer, appear linked to the polymetallic mineralization. Therefore, four samples of this type of calcite vein including white and black calcite veins were also collected (e.g., Fig. 3a, Supplementary Materials). Third, three other calcite veins, closely intercalated within the polymetallic Ni–Mo–PGE sulfide ores, were investigated together along with seven REE data from Feng et al. (2011) (Fig. 3e, Supplementary Materials). All samples of coarse-grained limestone and calcite veins were prepared to determine the trace elements, REE concentrations and Sr isotopic signature. Moreover several dolostone samples with abundant veins were collected from the Dengying Formation in Zhongnan villiage of Zunyi County for petrographic observation (Fig. 3f–h). Finally, the above-mentioned samples were prepared as polished sections.

Petrological investigations of polished sections were performed at the State Key Laboratory of Ore Deposit Geochemistry (SKLODG), Institute of Geochemistry, Chinese Academy of Sciences (IGCAS), using a JEOL JSM-7800FX field emission scanning electronic microscope (FESEM) with an EDAX energy dispersive X-ray spectroscope (EDS).

REE and several trace element concentrations were determined using a Perkin-Elmer Sciex ELAN DRC-e ICP-MS at the SKLODG, IGCAS. First, a 50 mg powder sample was dissolved in a high-pressure Teflon bombs with HF and HNO_3 at 190 °C for 48 h. Second, the residue was dissolved again with the appropriate amount of H_2O, HNO_3 and Rh at 145 °C for 12 h. Rh was used as an internal standard to monitor drift during the analysis (Qi et al., 2000). The standard reference materials AGV-2, AMH-1 and GBPG-1 were dissolved and measured together with our samples and the analytical precision was better than 10 % relative standard deviation. In particular, the absence of correlation between Ba and Eu anomalies in these studied samples suggests that there was no isobaric interference of BaO with Eu during the ICP-MS analytical procedure (Supplementary Materials).

Sr isotope separation was also carried out at the SKLODG, IGCAS. Given the measured $^{87}Sr/^{86}Sr$ can represent the initial $^{87}Sr/^{86}Sr$ of the calcite because of its extremely low Rb/Sr ratio and high Sr concentration, the limestone selectively dissolved by acetic acid (HAc) can be recommended for studies of the strontium isotopic curve during the Earth's history. In this study, similar experimental procedure was also carried out as follows (e.g., Derry et al., 1994; Nohda et al., 2013), to investigate the Sr isotopic signature of coarse-grained limestone and calcite veins. A 200 mg sample was dissolved with 10% HAc (blank values of Rb and Sr are 0.045 ppb and 1.05 ppb, respectively; Supplementary Materials) for six hours to dissolve the calcite, rather than silicate minerals, sulfides and barite, and the solution was centrifuged and filtered. After that, Sr was then separated using the standard ion exchange techniques (AG–50W–12X resin) with hydrochloric acid (HCl) purified by sub-boiling distillation. After separation, Sr isotope ratios were measured via a MAT262 solid isotope mass spectrometer at the Institute of Geology, Chinese Academy of Geological Sciences. All the results of $^{87}Sr/^{86}Sr$ were normalized to $^{88}Sr/^{86}Sr = 8.37521$. In this study, the $^{87}Sr/^{86}Sr$ ratio of the NBS987 ($SrCO_3$) was 0.710238 ± 0.000012 (2σ), consistent with the recommended value.

4. Results

4.1. Geological, mineralogical and petrographic results

There are two distinctly petrographic characteristics shown in coarse-grained limestone samples. One is that the quartz, illite, feldspar and pyrite are dispersed in the calcite matrix and at the interface of calcite grains (Fig. 4a). The other is that the quartz grains are surrounded by numerous micro granular apatite grains, together with a few sphalerite and pyrite grains dispersed in the calcite matrix (Fig. 4b).

Calcite veins vertically cut through coarse-grained limestone layer, but terminate in the overlying polymetallic sulfides layer. There are a number of dolomite and organic matter fragments with angular structure and pyrite occurring in these calcite veins (Fig. 4c and d). Moreover, in the organic matter fragments, many V-bearing and Ni-bearing sulfides also occur at the micro to nano scale (Fig. 4d). For another, the calcite veins intercalated in the polymetallic Ni–Mo–PGE sulfides layer are almost homogeneous, except for a few grains of sporadic Mo-bearing minerals (MoSC, Kao et al., 2001) and millerite (Fig. 4e–f). It is noteworthy that the Ni-bearing sulfides commonly host in these calcite veins.

In regards to the dolostone samples from the Dengying Formation in Zunyi area, two distinctive geological features are exhibited. One is the massive apatite associated with dispersed barite and dolomite grains, which fill in the fractures of the Dengying Formation dolostone (Figs. 3f, 4g). The other is that the Dengying Formation dolostone is cut through by the dolomite veins and barite-calcite veins (Figs. 3g–h, 4h).

4.2. Geochemical results

4.2.1. REE data

The REE and related trace elements data are listed in Supplementary Materials and REE patterns of coarse-grained limestone samples in Zunyi and Nayong areas are illustrated in Fig. 5a and b. For Zunyi area, the ∑REE ranges from 7.79 to 73.5 ppm, except for two high concentrations (152 ppm for ZNls-4 and 311 ppm for ZNls-5). The PAAS-normalized (post-Archean Australian shale; McLennan, 1989) REE patterns show significantly variable Eu anomalies (δEu), with values from 0.80 to 3.17 (Fig. 5a, Supplementary Materials). For Nayong area, the ∑REE mainly ranges from 21.8 to 79.2 ppm and δEu values vary from 0.85 to 1.61 (Fig. 5b, Supplementary Materials). Specifically, there are no significant variations of ∑REE and δEu in the lower and upper parts of coarse-grained limestone samples, such as ZNls-1, SDls-3 and SDls-6 (Fig. 3b, Supplementary Materials).

Calcite veins that cut through the coarse-grained limestone layer show extremely low ∑REE compared to those of coarse-grained limestone samples, which are from 0.31 to 4.74 ppm for white veins and from 0.82 to 16.0 ppm for black veins. Also, the PAAS-normalized REE patterns show positive Eu anomalies with δEu values from 1.91 to 94.2, but the abnormally high values may be attributed to extremely low concentration of Sm and Gd

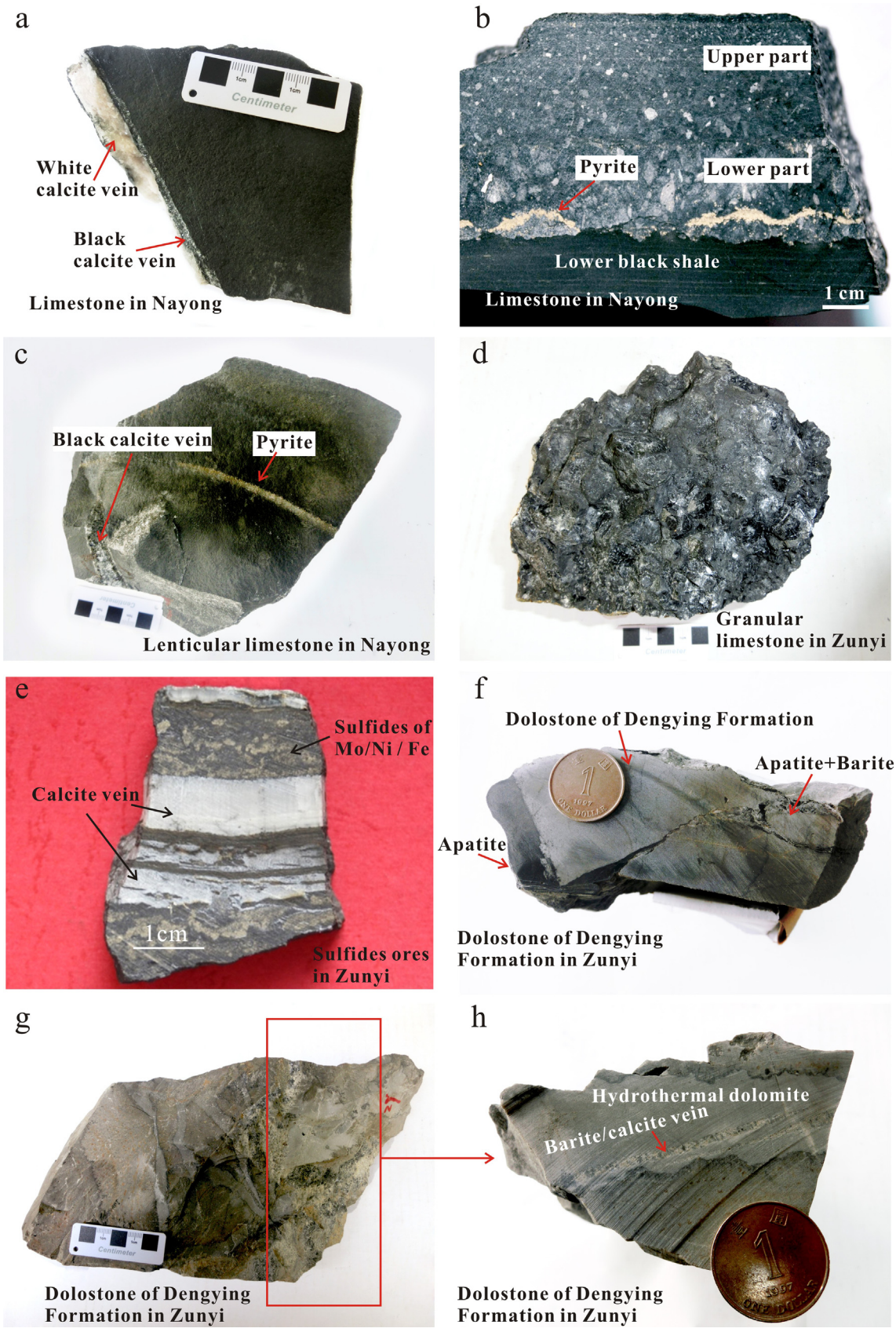

Fig. 3. Characteristics of the studied samples in Zhongnan villiage of Zunyi county (N 27°41′, E 106°40′) and Shuidong villiage of Nayong county (N 26°43′, E 105°33′), Guizhou Province, South China. a, b: coarse-grained limestone sample (Nayong) with stratiform structure and decreasing size of calcite grains from the lower part to upper part, which is often cut through by the calcite veins; c, d: coarse-grained limestone sample with lenticular (Nayong) and granular (Zunyi) structure; e: the calcite vein intercalated closely within the polymetallic sulfide ores (Zunyi); f: the dolostone of the Dengying Formation with massive apatite and barite filled in the fracture (Zunyi); g, h: the dolostone of the Dengying Formation which is cut through by latter hydrothermal dolomite and barite-calcite veins (Zunyi). The pictures were taken by Tao Han.

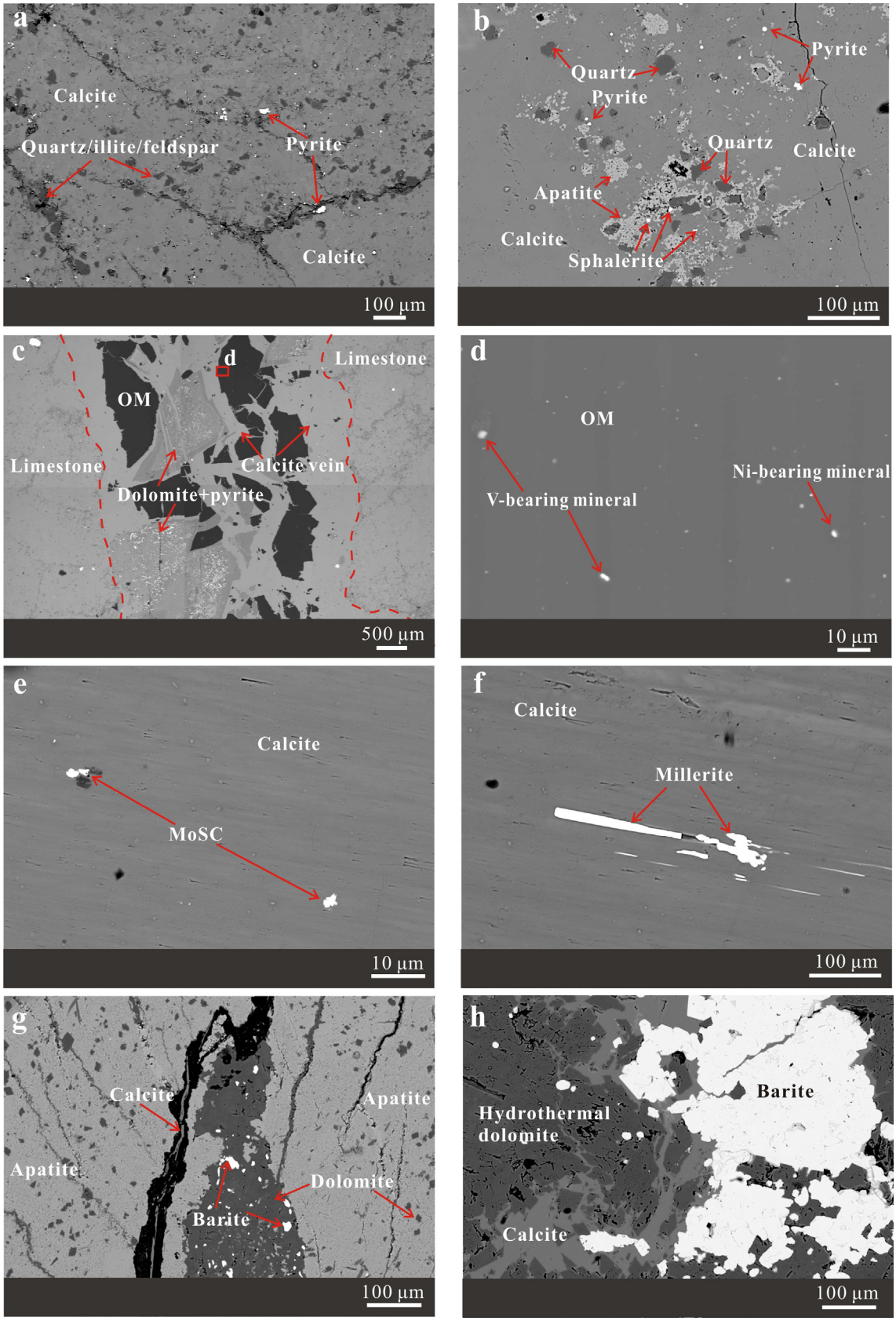

Fig. 4. Petrographic observations of studied samples by field emission scanning electronic microscope. a, b: two differently petrographic characteristics of coarse-grained limestone samples; c, d: the characteristics of calcite veins with dolomite and organic matter (OM) fragments with angular structure in coarse-grained limestone layer, d is the enlarged image in c; e. f: the characteristics of calcite vein in polymetallic sulfide ore; g, h: the characteristics of dolostone of the Dengying Formation with abundant calcite, apatite and barite minerals. The photographs were taken by Tao Han.

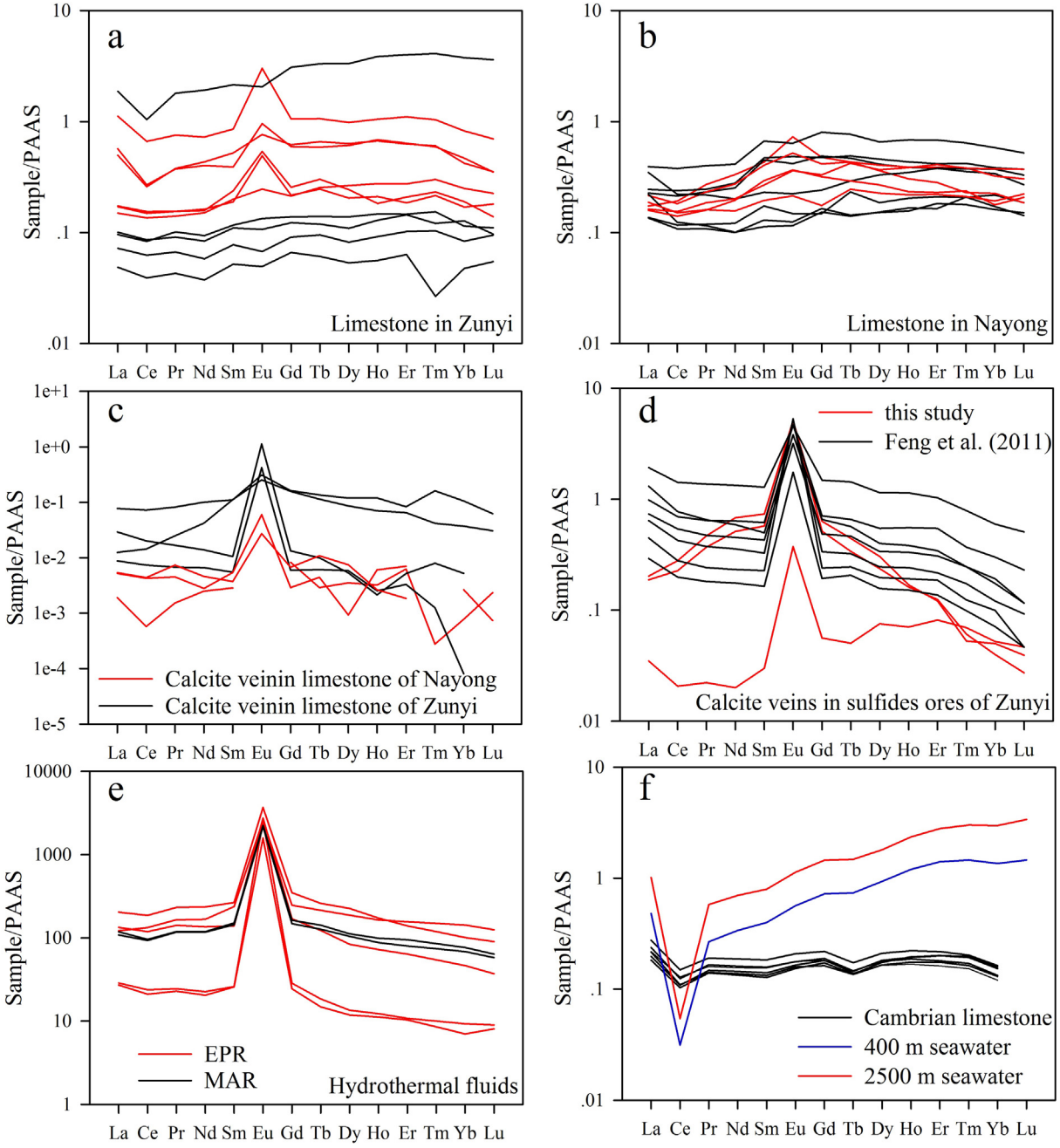

Fig. 5. PAAS-normalized REE patterns for coarse-grained limestone samples (a: Zunyi area; b: Nayong area); for calcite veins in coarse-grained limestone layer (c); for calcite veins intercalated within polymetallic sulfide ores (d); for hydrothermal fluids (data in pM) from Mid-Atlantic Ridge-MAR and East Pacific Rise-EPR (e; Douville et al., 1999); for present-day seawater (data in pM) and Cambrian limestone samples (f; Alibo and Nozaki, 1999; Ling et al., 2013). *Note:* the PAAS data (post-Archean Australian shale) are from McLennan (1989) and all the data are consistent with the Supplementary Materials.

during the δEu calculation and we just provide it for reference here (Fig. 5c, Supplementary Materials). Moreover, calcite veins intercalated in the polymetallic sulfides layer contribute to relatively high ∑REE concentrations ranging from 5.56 to 276 ppm. All positive Eu anomalies of these calcite veins with values from 3.29 to 22.7 are also exhibited in the PAAS-normalized REE patterns (Fig. 5d, Supplementary Materials).

4.2.2. Sr isotope data

The Sr isotope ratios of studied samples are also shown in Supplementary Materials. For instance, the initial $^{87}Sr/^{86}Sr$ values of coarse-grained limestone samples in Zunyi and Nayong areas are from 0.7088 to 0.7119 and from 0.7092 to 0.7126, respectively. Also, the Sr isotopic signatures are almost consistent in lower and upper parts of ZNls-1, SDls-3 and SDls-6 (Fig. 6; Supplementary Materials). In addition, both white and black calcite veins that cut through coarse-grained limestone layer show relatively high $^{87}Sr/^{86}Sr$ ratios ranging from 0.7083 to 0.7150 (Fig. 6; Supplementary Materials). Moreover, the $^{87}Sr/^{86}Sr$ ratios of calcite veins intercalated in polymetallic sulfides layer are relatively stable and range from 0.7112 to 0.7118 (Fig. 6; Supplementary Materials).

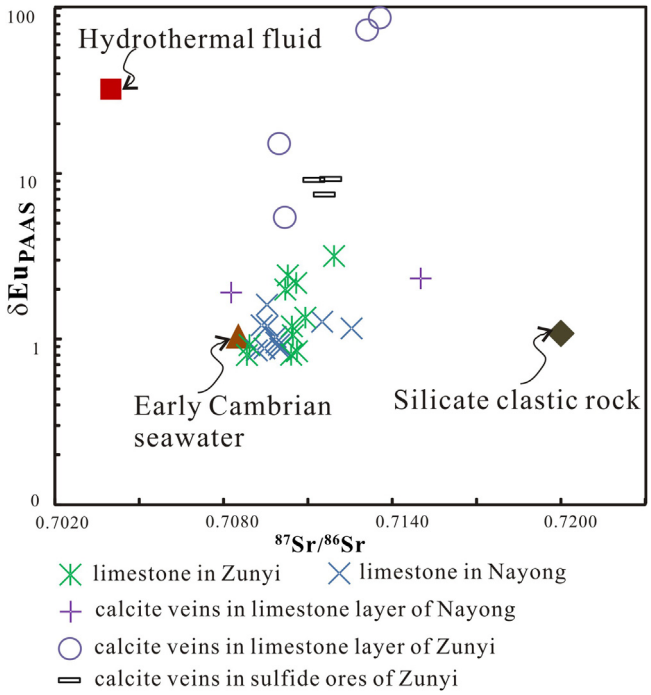

Fig. 6. Diagrams of Eu anomalies (δEu) against $^{87}Sr/^{86}Sr$ ratios for studied samples. The δEu and $^{87}Sr/^{86}Sr$ ratio of three end members are as follows: 1) hydrothermal fluids (δEu = 32, $^{87}Sr/^{86}Sr$ = 0.704) from Douville et al. (1999), Ravizza et al. (2001), and Amini et al. (2008); 2) Cambrian seawater (δEu = 1.04, $^{87}Sr/^{86}Sr$ = 0.7085) from Ling et al. (2013), Derry et al. (1994), Jacobsen and Kaufman (1999) and references therein; 3) silicate clastic rocks (δEu = 1.08, $^{87}Sr/^{86}Sr$ = 0.720) similar to upper continental crust from Rudnick and Gao (2003), and Faure (1977). *Note:* the abnormally high δEu values for the calcite veins in coarse-grained limestone layer might be due to their extremely low concentrations and provided here as a reference. All the data are consistent with the Supplementary Materials.

5. Discussion

5.1. Geochemical and geological implications for hydrothermal activity

5.1.1. REE geochemistry

In deep-sea hydrothermal systems, previous studies have proposed that REE concentrations of hydrothermal fluids are often controlled by the presence of plagioclase phenocrysts (e.g., Douville et al., 1999 and references therein). Hydrothermal fluids commonly contribute similar REE patterns and strikingly positive Eu anomalies in different tectonic settings (e.g., Mid-Atlantic Ridge and East Pacific Rise) where high temperature solutions percolate through the subsurface ultramafic/mafic rocks (e.g., Klinkhammer et al., 1994; Bau and Dulski, 1999; Douville et al., 1999; Fig. 5e). In this study, about half of coarse-grained limestone samples exhibit positive Eu anomalies, with δEu_{PAAS} values from 1.16 to 3.17, while the remainder yields δEu_{PAAS} values ranging from 0.80 to 1.05 (Fig. 5a and b; Supplementary Materials). These positive Eu anomalies are different from those of contemporaneous limestone (average δEu_{PAAS} = 1.04, Fig. 5f; Ling et al., 2013), present-day seawater (δEu_{PAAS} = 1.05, Alibo and Nozaki, 1999; Fig. 5f) and host black shale (δEu < 1, Jiang et al., 2006; Feng et al., 2011), but are similar to those of hydrothermal fluids with high values of δEu (δEu_{PAAS} = 10.6–93.0, Douville et al., 1999; Fig. 5e). In addition, the coexistence of positive and negative Eu patterns (0.80–3.17) are very consistent with those of the nearby polymetallic sulfide ores (0.60–2.78) and phosphate nodules (0.92–1.39) from the Niutitang Formation, which were proposed to be a result of submarine exhalative hydrothermal processes (Jiang et al., 2006; Zhu et al., 2014). Thus, by comparing the above-mentioned, positive Eu anomalies of coarse-grained limestone samples may also indicate the involvement of hydrothermal fluids during its formation, whereas the remainder without positive Eu anomalies may be weakly or not influenced by hydrothermal fluids. Coincidently, the mafic and ultramafic igneous rocks developed in South China during the Proterozoic era (Li and Gao, 2000) might be potential candidates for positive Eu anomalies related to hydrothermal process. In addition, these subsurface mafic and ultramafic rocks were similarly proposed as the source of PGE in overlying polymetallic Ni–Mo–PGE mineralization (Li and Gao, 2000; Han et al., 2015b). Therefore, the positive Eu anomalies of the coarse-grained limestone samples are indicative of remarkable hydrothermal activity during the early Cambrian which might be related to the Proterozoic mafic/ultramafic rocks.

Furthermore, the abnormally high δEu_{PAAS} values (up to 94.3) of calcite veins that cut through the coarse-grained limestone layer might be attributed to the extremely low concentration of Sm and Gd during the calculation of δEu_{PAAS}, but the remaining positive Eu anomalies (δEu_{PAAS} = 1.19–2.33; Fig. 5c; Supplementary Materials) are also presented. Positive Eu anomalies are also found in those calcite veins intercalated within the polymetallic sulfides layer (δEu_{PAAS} = 3.29–22.7, Fig. 5c and d; Supplementary Materials). As mentioned above, the calcite veins in coarse-grained limestone layer and polymetallic sulfides ores similarly also indicate the presence of hydrothermal activity and a possible linkage with the nearby polymetallic Ni–Mo–PGE mineralization.

5.1.2. Sr isotope geochemistry

The $^{87}Sr/^{86}Sr$ isotopic signature of seawater during the early Cambrian has been extensively determined to be near 0.7085 (e.g., Derry et al., 1994; Jacobsen and Kaufman, 1999; Sawaki et al., 2008 and references therein). In South China, the Sr isotopic excursion across the Precambrian–Cambrian boundary is characterized by a suddenly increase from 0.7087 to 0.7108 in the uppermost Ediacaran, and then a gradual decrease to 0.7090 in the lowermost Cambrian in the Three Gorges area (Sawaki et al., 2008). Recently, Li et al. (2013) proposed the Sr isotope evolution of seawater, which shows a decreasing trend from 0.7085–0.7086 to 0.7082–0.7083 across the Ediacaran–Cambrian transition from the Xiaotan section, Yunnan Province. On the contrary, it has been proposed that the mafic/ultramafic-hosted submarine hydrothermal fluids from the East Pacific Rise and Mid-Atlantic Ridge often exhibit relatively smaller values from 0.7034 to 0.7042 in marine environments (e.g., Ravizza et al., 2001; Amini et al., 2008). Nevertheless, in this study, the initial $^{87}Sr/^{86}Sr$ values of almost all coarse-grained limestone samples (0.7088–0.7126, Fig. 6; Supplementary Materials) are higher than those of early Cambrian seawater and modern hydrothermal fluids. Furthermore, much higher initial $^{87}Sr/^{86}Sr$ isotope values are also obtained from the calcite veins of coarse-grained limestone layer (0.7083–0.7150, Fig. 6; Supplementary Materials) and the calcite veins of polymetallic sulfides ores (0.7112–0.7118, Fig. 6; Supplementary Materials). Meanwhile, higher initial $^{87}Sr/^{86}Sr$ values ranging from 0.7087 to 0.7123 were also found in the phosphate nodules from the lower Cambrian Niutitang Formation, NW Hunan Province (Zhu et al., 2014). Žák et al. (2003) also suggested a higher Sr isotope ratio (e.g., 0.7167) for the accessory barite in the polymetallic sulfides layer at the Zunyi area which may be caused by either hydrothermal fluid derived from older Precambrian crust or younger hydrothermal event. By comparing these higher Sr isotopic signatures, it appears that there is another source of enriched radiogenic Sr involved in the formation of coarse-grained limestone layer, as well as in the calcite veins of coarse-grained limestone and polymetallic sulfides layer. It is well known that silicate clastic rocks with $^{87}Sr/^{86}Sr$ values up to 0.72 may be the most suitable candidates (Faure, 1977 and references therein). Combined with the

positive Eu anomalies, it is likely that the hydrothermal fluid flowing through the silicate clastic rocks could contribute higher $^{87}Sr/^{86}Sr$ values detected in the studied samples. In fact, the involvement of enriched radiogenic Sr was often found in some economic deposits related to hydrothermal systems in South China, in which these higher $^{87}Sr/^{86}Sr$ values were interpreted as hydrothermal fluids interacting with the silicate clastic rocks from the basement or the wall rocks, such as the Xujiashan antimony deposit hosted by the marine carbonates of the Ediacaran Doushantuo and Dengying Formations, the Kangdian IOCG (Iron Oxide Copper Gold) metallogenic province hosted by the Paleoproterozoic volcanic-sedimentary succession and the Zn–Pb deposits hosted by the dolostone of the Ediacaran Dengying Formation and the lower Cambrian Meishucun/Qingxudong Formations (Schneider et al., 2002; Shen et al., 2010; Chen et al., 2014; Zhao et al., 2015; Zhou et al., 2015a).

As a consequence, integrating end members of the Cambrian seawater, hydrothermal fluids and silicate clastic rocks for δEu and initial $^{87}Sr/^{86}Sr$ in Fig. 6, it appears that the positive Eu anomalies and enriched radiogenic Sr of studied samples may be inherited from the hydrothermal fluid derived from the Proterozoic mafic/ultramafic rocks and the underlying Precambrian silicate clastic rocks (e.g., Xiajiang, Banxi or Lengjiaxi Groups, Wang et al., 2015b).

5.1.3. Geological evidence of hydrothermal activity

Quite apart from the geochemical evidence for hydrothermal activity, there are geological features that also point out the potential occurrence of multi-stage hydrothermal activity during the early Cambrian in South China. As mentioned above, a large number of calcite veins, whether cutting through the coarse-grained limestone layer or intercalated with the polymetallic sulfide ores, suggest widespread development involvement of hydrothermal fluids. Specifically, numerous dolomite and organic matter fragments with angular structure were incorporated into the calcite veins of coarse-grained limestone layer. These dolomite fragments contain abundant co-genetic pyrite grains similarly indicating hydrothermal modification (Fig. 4c). Also, these hydrothermal calcite veins are likely connected with adjacent polymetallic sulfide layer based on the presence of Ni-bearing sulfides they all have (Fig. 4d, f; Han et al., 2015b). Furthermore, abundant hydrothermal veins, including the dolomite and barite-calcite assemblages in the dolostone of the Dengying Formation, similarly show hydrothermal activity during this critical geological period (Figs. 3f–h, 4g–h). These hydrothermal dolomite and barite-calcite veins could be correlate with the hydrothermal dolostone and/or dolomitization in the Dengying Formation and the bedded stratiform barite deposits in the Niutitang Formation of Guizhou and Hunan Provinces (e.g., Liu et al., 2014; Han et al., 2015a and references therein). In addition to this, abundant chert precipitated along the southern margin of the Yangtze platform occurring in the form of mounted, veined, brecciated and bedded structures, was also attributed to low temperature, silica-rich hydrothermal systems (Chen et al., 2009; Wang et al., 2012; Fan et al., 2013). Finally, it should be noted that these diverse veins occur within the lower Cambrian has not been accurately dated. Nonetheless, it is likely that multi-stage submarine hydrothermal activity took place during the early Cambrian in South China.

5.2. Hydrothermal contribution to the mineralization/ore deposits

For the lower Cambrian of the Yangtze Platform, South China, previous investigators have proposed that hydrothermal contribution may play an important role in the extreme metal accumulations in several metal-enriched deposits (e.g., Ni, Mo, Se, PGE, Ba, Si). Despite a long-running debate, it has not been conclusively determined whether the metal enrichment was due to hydrothermal origin or seawater scavenging (e.g., Coveney and Chen, 1991; Mao et al., 2002; Jiang et al., 2006, 2007; Lehmann et al., 2007, 2016). Here, the polymetallic Ni-Mo-PGE mineralization and the barite deposits were taken as examples based on our results and previous studies to evaluate the possibility of the hydrothermal contributions. The former is an unusual thin bed that is hosted in the lowermost Cambrian of the Yangtze Platform and has received extensive attention during the past four decades (Coveney and Pašava, 2005). The latter is one of the most important areas globally for barite exploration, with reserves of at least 200 million tonnes (Yang et al., 2008).

5.2.1. Polymetallic Ni-Mo-PGE mineralization

As discussed in previous studies, whether the metals are of submarine hydrothermal origin or scavenging from seawater is the main focus of debate for the polymetallic Ni-Mo-PGE mineralization. Initially, Fan (1983) proposed the polymetallic Ni–Mo–PGE sulfides ores are attributed to extraterrestrial impact based on the Ir anomaly (11–31 ppb). Coveney and Chen (1991) suggested that the Ni-Mo-PGE sulfides beds probably originated from submarine springs through deep fractures during the Cambrian, according to the linear distribution of the known ore deposits. Studies of fluid inclusions associated with the sulfide ores and S isotopes of the pyrite nodules indicate that the metal sulfide mineralization was attributed to the variable salinity hydrothermal fluids, with some ore constituents introduced into a bacteriogenic sulfide-rich environment (Murowchick et al., 1994; Lott et al., 1999). Nevertheless, new evidence for the seawater origin has also been suggested. That is to say, the element concentration pattern of the polymetallic sulfides ores is similar, but is exceptionally enriched by factors of $\sim 10^7$ compared to modern seawater, which may have formed in a sediment-starved, stratified basin with replenishment by fresh seawater and euxinic deep water (Mao et al., 2002; Lehmann et al., 2007). Additionally, the integrated geochemical evidence, including Mo and Cr isotopes, PGE, trace and rare earth elements, suggest that most metals of the polymetallic sulfide ores were scavenged from early Cambrian seawater (Xu et al., 2012b; Lehmann et al., 2016). Beyond that, Kříbek et al. (2007) considered that polymetallic sulfides layer represent a remnant of phosphate- and sulfide-rich subaquatic hardground supplied with organic material derived from plankton and benthic communities as well as with algal/microbial oncolite-like bodies that originated in wave-agitated, shallow-water, nearshore environment. Simultaneously, the submarine hydrothermal origin has been suggested as well, based on the PGE, REE patterns and Sr isotope (Li and Gao, 2000; Žák et al., 2003; Jiang et al., 2006, 2007; Orberger et al., 2007) and also comparision with Ba-deposits (Pašava et al., 2008). In addition, the Se isotope and Se speciation studies consistently note the hydrothermal contribution for the Se accumulation in this polymetallic Ni-Mo-Se sulfide layer (Fan et al., 2011; Wen and Carignan, 2011). Recently, the results of trace elements and PGE in Nayong area, Guizhou Province suggested that multiple metal sources may be responsible for the formation of polymetallic Ni–Mo–PGE mineralization. Namely, the Proterozoic and Early Palaeozoic mafic and ultramafic rocks, dolomites and/or Pb–Zn deposits of the Neoproterozoic Dengying Formation and seawater could be the principal sources for Co–Ni–Cu–PGE, Zn–Cd–Pb, and Mo–Tl–TOC, respectively (Han et al., 2015b). This conclusion was consistent with other recent studies that also suggest different sources and enrichment mechanisms for Ni and Mo (Cao et al., 2013; Shi et al., 2014; Han et al., 2014).

Reasons for these uncertainties and contradictions may be mainly due to the complicated elemental associations, such as elements associated with felsic rocks (Mo–Pb–Zn–REE) and elements associated with mafic/ultramafic rocks (Fe–Ni–Cu–PGE), which

makes distinguishing their origins and sources difficult. In this study, the coarse-grained limestone layer and related calcite veins in Zunyi and Nayong areas, Guizhou Province further indicate the most likely occurrence of hydrothermal contribution for the polymetallic Ni–Mo–PGE mineralization. Combined with our recent studies (Han et al., 2015b), this study suggests that there is a significant hydrothermal contribution with relatively high temperature, low-pH, and Cl-rich fluids for the metal accumulation, such as Ni, Zn and PGE during the formation of polymetallic Ni–Mo–PGE mineralization, despite the probable seawater scavenging for extreme Mo enrichment.

5.2.2. Barium ore deposits

The distinctive black shale or chert hosted stratiform barium deposits that are mainly distributed along the north and south margins of the Yangtze Platform have led China to become one of the largest barium producers in the world. This type of barium mineralization mainly occurs in the lower Cambrian, which is underlain by phosphorite and overlain by black shale. It is usually in the form of barite and witherite deposits, with massive, laminated, banded and nodular textures for the barite deposits, and compact, massive and nodular textures for the witherite deposits (Wang and Li, 1991). Within the scope of our study, the significant barite deposits that occur in Tianzhu, Guizhou Province and Xinhuang, Hunan Province are characterized (Fig. 1).

Many previous studies have suggested that hydrothermal process is the main cause of barite mineralization in Guizhou and Hunan Provinces. For instance, many algae, sponge spicules and tube-type fossils well-preserved in the barite sequences present a scene of a hydrothermal venting community thriving in the hydrothermal system during the early Cambrian (Yang et al., 2008). Žák et al. (2003) and Pašava et al. (2008) advocated an hydrothermal origin of barite deposits in the eastern part of Guizhou Province describing hydrothermal channels for Ba-mineralization. Additionally, a hydrothermal-related mineral, hyalophane, with zoned texture was detected and investigated only in the ore horizon, which indicates that barite mineralization may result from fault-controlled multi-stage hydrothermal activity (Han et al., 2015a; Xia et al., 2004). Furthermore, the positive Eu anomalies of the mineralized horizon (3.23–8.40) are higher than those of the nearby non-mineralized horizon (1.06–1.42), and indicate that the hydrothermal activity mainly contributed to the barite deposit (Han et al., 2015a), but it is not sure whether there is the isobaric interference of BaO with Eu during the ICP-MS analysis because of the extremely high Ba concentration. For the other, the Sr isotope analysis, the most feasible geochemical indicator for distinguishing marine barite and hydrothermal barite, was also applied to these deposits (Paytan et al., 2002; Wang and Chu, 1993; Xia et al., 2004; Žák et al., 2003). In South China, the Sr isotope ratios of the barite deposits, have most values (0.7083–0.7087) lower than that of Cambrian seawater but similar to those of the submarine hydrothermal system (0.7034 to 0.7042; Ravizza et al., 2001; Amini et al., 2008). It was proposed that these lower $^{87}Sr/^{86}Sr$ ratios of barite deposits may derived from a submarine hydrothermal vent/volcano during its formation (Wang and Chu, 1993; Xia et al., 2004). However, these lower initial $^{87}Sr/^{88}Sr$ values should be further evaluated as well as they could be related to the dissolution technique used during the Sr isotope determination. The lower $^{87}Sr/^{86}Sr$ ratios of the barite deposits were obtained from the dissolution by mixing reagents of HF, HCl, HNO_3 and $HClO_4$ in South China (Wang and Chu, 1993; Xia et al., 2004), which were different from the traditional barite-selective dissolution technique of alkali fusion with Na_2CO_3 or the resin chelation method used in other Sr isotope determinations of barite (Martin et al., 1995; Paytan et al., 2002; Zhou et al., 2015b). Thus, in view of the uncertain evidence of hydrothermal activities for the barite deposits in South China, further studies using appropriate geochemical techniques should be conducted to constrain the mineralization process of these significant barite deposits.

6. Conclusions

This study suggests that the coarse-grained limestone layer just below the polymetallic Ni–Mo–PGE sulfides layer, is a marine carbonate rock with remarkable alteration by hydrothermal fluid, and provides the best evidence of hydrothermal contribution to the polymetallic mineralization based on the petrographic observations, positive Eu anomalies, and higher $^{87}Sr/^{86}Sr$ ratios during the early Cambrian, South China. In addition, widespread calcite veins in coarse-grained limestone layer and polymetallic sulfide ores, with positive Eu anomalies and higher initial $^{87}Sr/^{86}Sr$ ratios also point out the development of a hydrothermal activity. The common Ni-bearing sulfides in these calcite veins and polymetallic sulfides ores further indicate an hydrothermal contribution for the polymetallic Ni–Mo–PGE mineralization. In particular, hydrothermal activity with relatively high temperature, low-pH, and Cl-rich fluids, which might have originated from the subsurface mafic/ultramafic rocks and flowed through Precambrian basement silicate clastic rocks, may be prevalent and play an important role in extreme element accumulation during the early Cambrian in South China. Finally, with the addition of the abundant hydrothermal dolomite and barite-calcite veins of the Dengying Formation, it appears that there were multi-stage activities with varied fluid compositions that developed widely across the Ediacaran–Cambrian transition in South China.

Acknowledgments

This project was supported by the National Natural Science Foundation of China (Grant Nos. 41303039, 41573011), the National Basic Research Program of China (2014CB440906), the Youth Innovation Promotion Association of the Chinese Academy of Sciences (2015), the CAS "Light of West China" Program (2014). We give many thanks to Jing Hu, Yan Huang, Suohan Tang for determining the trace element and Sr isotope, to Dr. Zhenghang Lv and Kunyue Ling for helping in the field work, to Prof. Steve Barnes and Dr. Anais Pagès (CSIRO-Mineral resources, Australia) for their revisions on this paper, to Profs. Coveney and Pašava, and another anonymous reviewer for reviewing and improving this paper.

Appendix A. Supplementary data

Supplementary data associated with this article can be found, in the online version, at http://dx.doi.org/10.1016/j.oregeorev.2017.02.030.

References

Alibo, D.S., Nozaki, Y., 1999. Rare earth elements in seawater: particle association, shale-normalization, and Ce oxidation. Geochim. Cosmochim. Acta 63, 363–372.

Amini, M., Eisenhauer, A., Böhm, F., Fietzke, J., Bach, W., Garbe-Schönberg, A., Rosner, M., Bock, B., Lackschewitz, K.S., Hauff, F., 2008. Calcium isotope ($\delta^{44/40}Ca$) fractionation along hydrothermal pathways, Logatchev field (Mid-Atlantic Ridge, 14°45'N). Geochim. Cosmochim. Acta 72, 4107–4122.

Baross, J.A., Hoffman, S.E., 1985. Submarine hydrothermal vents and associated gradient environment as sites for the origin and evolution of life. Orig. Life Evol. Biosph. 15, 327–345.

Bau, M., Dulski, P., 1999. Comparing yttrium and rare earths in hydrothermal fluids from the Mid-Atlantic Ridge: implications for Y and REE behavior during near-vent mixing and for the Y/Ho ratio of Proterozoic seawater. Chem. Geol. 155, 77–90.

Cai, C., Xiang, L., Yuan, Y., He, X., Chu, X., Chen, Y., Xu, C., 2015. Marine C, S and N biogeochemical processes in the redox-stratified early Cambrian Yangtze Ocean. J. Geol. Soc. 172, 390–406.
Cao, J., Hu, K., Zhou, J., Shi, C.H., Bian, L.Z., Yao, S.P., 2013. Organic clots and their differential accumulation of Ni and Mo within early Cambrian black-shale-hosted polymetallic Ni–Mo deposits, Zunyi, South China. J. Asian Earth Sci. 62, 531–536.
Chen, D.Z., Wang, J.G., Qing, H.R., Yan, D.T., Li, R.W., 2009. Hydrothermal venting activities in the Early Cambrian, South China: petrological, geochronological and stable isotopic constraints. Chem. Geol. 258, 168–181.
Chen, J.Y., Yang, R.D., Wei, H.R., Gao, J.B., 2013. Rare earth element geochemistry of Cambrian phosphorites from the Yangtze Region. J. Rare Earths 31, 101–112.
Chen, W.T., Zhou, M.F., Gao, J.F., 2014. Constraints of Sr isotopic compositions of apatite and carbonates on the origin of Fe and Cu mineralizing fluids in the Lala Fe-Cu-(Mo, LREE) deposit, SW China. Ore Geol. Rev. 61, 96–106.
Chen, D.Z., Zhou, X.Q., Fu, Y., Wang, J.G., Yan, D.T., 2015. New U-Pb zircon ages of the Ediacaran-Cambrian boundary strata in South China. Terra Nova 27, 62–68.
Cheng, M., Li, C., Zhou, L., Algeo, T.J., Zhang, F.F., Romaniello, S., Jin, C.S., Lei, L.D., Feng, L.J., Jiang, S.Y., 2016. Marine Mo biogeochemistry in the context of dynamically euxinic mid-depth waters: a case study of the lower Cambrian Niutitang shales, South China. Geochim. Cosmochim. Acta 183, 79–93.
Coveney Jr., R.M., Chen, N.S., 1991. Ni–Mo–PGE–Au-rich ores in Chinese black shales and speculations on possible analogues in the United States. Miner. Deposita 26, 83–88.
Coveney Jr., R.M., Pašava, J., 2005. Origins of Au-Pt-Pd-bearing Ni-Mo-As-(Zn) deposits hosted by Chinese black shales. In: Mao, J. (Ed.), Proceedings of the 8th Biennial SGA Meeting, Beijing Mineral Deposits Research: Meeting the Global Challenge, China, vol. 1. Springer, Heidelberg, pp. 101–102.
Derry, L.A., Brasier, M.D., Corfield, R.M., Rozanov, A.Y., Zhuravlev, A.Y., 1994. Sr and C isotopes in Lower Cambrian carbonates from the Siberian craton: a paleoenvironmental record during the "Cambrian explosion". Earth Planet. Sci. Lett. 128, 671–681.
Douville, E., Bienvenu, P., Charlou, J.L., Donval, J.P., Fouquet, Y., Appriou, P., Gamo, T., 1999. Yttrium and rare earth elements in fluids from various deep-sea hydrothermal systems. Geochim. Cosmochim. Acta 63, 627–643.
Emsbo, P., Hofstra, A.H., Johnson, C.A., Koenig, A., Grauch, R., Zhang, X.C., Hu, R.Z., Su, W.C., Pi, D.H., 2005. Lower cambrian metallogenesis of south China: interplay between diverse basinal hydrothermal fluids and marine chemistry. In: Mao, J. W., Bierlein, F.P. (Eds.), Mineral Deposit Research: Meeting the Global Challenge. Springer, New York, pp. 115–118.
Fan, D.L., 1983. Polyelements in the Lower Cambrian black shale series in southern China. In: Augustithis, S.S. (Ed.), The Significance of Trace Elements in Solving Petrogenetic Problems and Controversies. Theophrastus Publications S. A, Athens, pp. 447–474.
Fan, H.F., Wen, H.J., Hu, R.Z., Zhao, H., 2011. Selenium speciation in Lower Cambrian Se-enriched strata in South China and its geological implications. Geochim. Cosmochim. Acta 75, 7725–7740.
Fan, H.F., Wen, H.J., Zhu, X.K., Hu, R.Z., Tian, S.H., 2013. Hydrothermal activity during Ediacaran-Cambrian transition: silicon isotopic evidence. Precambr. Res. 224, 23–35.
Fang, W.X., Hu, R.Z., Su, W.C., Qi, L., Xiao, J.F., Jiang, G.H., 2002. Geochemical characteristics of Dahebian-Gongxi superlarge barite deposits and analysis on its background of tectonic geology, China. Acta Petrol. Sinica 18, 247–256.
Faure, G., 1977. Principles of Isotope Geology. John Wiley & Sons, New York.
Feng, Z.Z., Peng, Y.M., Jin, Z.K., Bao, Z.D., 2002. Lithofacies palaeogeography of the early Cambrian in China. J. Palaeogeogr. 4, 1–14 (in Chinese with English abstract).
Feng, C.X., Chi, G.X., Hu, R.Z., Liu, S., Liu, J.J., Luo, T.Y., Qi, Y.Q., 2011. Feature of ore-forming fluid: evidence from fluid inclusion, REE and carbon-oxygen isotope geochemistry of calcite from Huangjiawan Mo–Ni polymetallic ore deposits, Zunyi, Guizhou province. Acta Petrol. Sinica 27, 3763–3776 (in Chinese with English abstract).
Feng, L.J., Li, C., Huang, J., Chang, H.J., Chu, X.L., 2014. A sulfate control on marine mid-depth euxinia on the early Cambrian (ca. 529–521Ma) Yangtze platform, South China. Precambrian Res. 246, 123–133.
Gao, J.B., Wei, H.R., Liu, K., Tan, D.W., Yang, R.D., 2011. Sedimentary features of molybdenum-nickel-bearing strata in the Cambrian black rock series in Zunyi-Nayong area, Guizhou province. Geol. Resour. 20, 234–239 (in Chinese with English abstract).
Guo, Q.J., Deng, Y.N., Hippler, D., Franz, G., Zhang, J.M., 2016. REE and trace element patterns from organic-rich rocks of the Ediacaran-Cambrian transitional interval. Gondwana Res. 36, 81–93.
Han, S.C., Hu, K., Cao, J., Pan, J.Y., Liu, Y., Bian, L.Z., Shi, C.H., 2014. Mineralogy of early Cambrian Ni-Mo polymetallic black shale at the Sancha Deposit, South China: implications for ore genesis. Resour. Geol. 65, 1–12.
Han, S.C., Hu, K., Cao, J., Pan, J.Y., Xia, F., Wu, W.F., 2015a. Origin of early Cambrian black-shale-hosted barite deposits in South China: mineralogical and geochemical studies. J. Asian Earth Sci. 106, 79–94.
Han, T., Zhu, X.Q., Li, K., Jiang, L., Zhao, C.H., Wang, Z.G., 2015b. Metal sources for the polymetallic Ni–Mo–PGE mineralization in the black shales of the Lower Cambrian Niutitang Formation, South China. Ore Geol. Rev. 67, 158–169.
Hu, N.Y., Xia, H.D., Dai, T.G., You, X.J., Bao, Z.X., Bao, J.M., 2010. Sedimentary vanadium deposit of lower Cambrian black rock series in western Hunan. Contr. Geol. Mineral Resour. Res. 25, 296–302 (in Chinese with English abstract).
Jacobsen, S.B., Kaufman, A.J., 1999. The Sr, C and O isotopic evolution of Neoproterozoic seawater. Chem. Geol. 161, 37–57.
Jiang, S.Y., Chen, Y.Q., Ling, H.F., Yang, J.H., Feng, H.Z., Ni, P., 2006. Trace- and rare-earth element geochemistry and Pb–Pb dating of black shales and intercalated Ni–Mo–PGE–Au sulfide ores in Lower Cambrian strata, Yangtze Platform, South China. Miner. Deposita 41, 453–467.
Jiang, S.Y., Yang, J.H., Ling, H.F., Chen, Y.Q., Feng, H.Z., Zhao, K.D., Ni, P., 2007. Extreme enrichment of polymetallic Ni–Mo–PGE–Au in lower Cambrian black shales of South China: an Os isotope and PGE geochemical investigation. Palaeogeogr. Palaeoclimatol. Palaeoecol. 254, 217–228.
Jiang, S.Y., Pi, D.H., Heubeck, C., Frimmel, H., Liu, Y.P., Deng, H.L., Ling, H.F., Yang, J.H., 2009. Early Cambrian ocean anoxia in South China. Nature 459, E5–6.
Jin, H.X., Li, J.Q., Wang, H., 2007. Distribution of REE of phosphate concentrate in wet-phosphoric acid process. J. Rare Earths 25, 78–84.
Jin, C.S., Li, C., Algeo, T.J., Planavsky, N.J., Cui, H., Yang, X.L., Zhao, Y.L., Zhang, X.L., Xie, S.C., 2016. A highly redox-heterogeneous ocean in South China during the early Cambrian (~529–514 Ma): implications for biota-environment co-evolution. Earth Planet. Sci. Lett. 441, 38–51.
Kao, L.S., Peacor, D.R., Coveney Jr., R.M., Zhao, G.M., Dungey, K.E., Curtis, M.D., Penner-Hahn, J.E., 2001. A C/MoS2 mixed-layer phase (MoSC) occurring in metalliferous black shales from southern China, and new data on jordisite. Am. Mineral. 86, 852–861.
Klinkhammer, G.P., Elderfield, H., Edmond, J.M., Mitra, A., 1994. Geochemical implications of rare earth element patterns in hydrothermal fluids from mid-ocean ridges. Geochim. Cosmochim. Acta 58, 5105–5113.
Kříbek, B., Sýkorová, I., Pašava, J., Machovič, V., 2007. Organic geochemistry and petrography of barren and Mo-Ni- PGE mineralized marine black shales of the Lower Cambrian Niutitang Formation (south China). Int. J. Coal Geol. 72, 240–256.
Lehmann, B., Nagler, T.F., Holland, H.D., Wille, M., Mao, J.W., Pan, J.Y., Ma, D.S., Dulski, P., 2007. Highly metalliferous carbonaceous shale and Early Cambrian seawater. Geology 35, 403–406.
Lehmann, B., Frei, R., Xu, L.G., Mao, J.W., 2016. Early Cambrian black shale-hosted Mo-Ni and V mineralization on the rifted margin of the Yangtze Platform, China: reconnaissance chromium isotope data and a refined metallogenic model. Econ. Geol. 111, 89–103.
Li, Y.Y., 1997. The geological characteristics of sea-floor exhalation-sedimentary chert in Lower Cambrian Black Shales in Dayong-Cili Area, Hunan Province. Act Petrol. Sinica 13, 121–126 (in Chinese with English abstract).
Li, S.R., Gao, Z.M., 2000. Source tracing of noble metal elements in Lower Cambrian black rock series of Guizhou-Hunan Provinces, China. Sci. China Earth Sci. 43, 625–632.
Li, D., Ling, H.F., Shields-Zhou, G.A., Chen, X., Cremonese, L., Och, L., Thirlwall, M., Manning, C.J., 2013. Carbon and strontium isotope evolution of seawater across the Ediacaran-Cambrian transition: evidence from the Xiaotan section, NE Yunnan, South China. Precambr. Res. 225, 128–147.
Ling, H.F., Chen, X., Li, D., Wang, D., Shields-Zhou, G.A., Zhu, M.Y., 2013. Cerium anomaly variations in Ediacaran–earliest Cambrian carbonates from the Yangtze Gorges area, South China: implications for oxygenation of coeval shallow seawater. Precambr. Res. 225, 110–127.
Liu, S.G., Huang, W.M., Jansa, L.F., Wang, G.Z., Song, G.Y., Zhang, C.J., Sun, W., Ma, W. X., 2014. Hydrothermal dolomite in the upper Sinian (upper Proterozoic) Dengying Formation, east Sichuan Basin, China. Acta Geol. Sinica 88, 1466–1487 (English Edition).
Liu, Z.H., Zhuang, X.G., Teng, G.E., Xie, X.M., Yin, L.M., Bian, L.Z., Feng, Q.L., Algeo, T.J., 2015. The lower Cambrian Niutitang Formation at Yangtiao (Guizhou, SW China): organic matter enrichment, source rock potential and hydrothermal influences. J. Pet. Geol 38, 411–432.
Lott, D.A., Coveney Jr., R.M., Murowchick, J.B., Grauch, R.I., 1999. Sedimentary exhalative nickel–molybdenum ores in South China. Econ. Geol. 94, 1051–1066.
Mao, J.W., Lehmann, B., Du, A.D., Zhang, G.D., Ma, D.S., Wang, Y.T., Zeng, M.G., Kerrich, R., 2002. Re–Os dating of polymetallic Ni–Mo–PGE–Aumineralization in lower Cambrian black shales of south China and its geologic significance. Econ. Geol. 97, 1051–1061.
Martin, E.E., Macdougall, J.D., Herbert, T.D., Paytan, A., Kastner, M., 1995. Strontium and neodymium isotopic analyses of marine barite separates. Geochim. Cosmochim. Acta 59, 1353–1361.
Mcdermott, J.M., Seewald, J.S., German, C.R., Sylva, S.P., 2015. Pathways for abiotic organic synthesis at submarine hydrothermal fields. Proc. Natl. Acad. Sci. U.S.A. 112, 7668–7672.
McLennan, S.M., 1989. Rare-earth elements in sedimentary-rocks – influence of provenance and sedimentary processes. Rev. Mineral. 21, 169–200.
Murowchick, J.B., Coveney Jr., R.M., Grauch, R.I., Eldridge, C.S., Shelton, K.L., 1994. Cyclic variations of sulfur isotopes in Cambrian stratabound Ni–Mo–(PGE–Au) ores of southern China. Geochim. Cosmochim. Acta 58, 1813–1823.
Nisbet, E.G., Sleep, N.H., 2001. The habitat and nature of early life. Nature 409, 1083–1091.
Nohda, S., Wang, B.S., You, C.F., Isozaki, Y., Uchio, Y., Buslov, M.M., Maruyama, S., 2013. The oldest (Early Ediacaran) Sr isotope record of mid-ocean surface seawater: chemostratigraphic correlation of a paleo-atoll limestone in southern Siberia. J. Asian Earth Sci. 77, 66–76.
Och, L.M., Cremonese, L., Shields-Zhou, G.A., Poulton, S.W., Struck, U., Ling, H.F., Li, D., Chen, X., Manning, C., Thirlwall, M., Strauss, H., Zhu, M., 2015. Palaeoceanographic controls on spatial redox distribution over the Yangtze Platform during the Ediacaran-Cambrian transition. Sedimentology 63, 378–410.
Orberger, B., Vymazalova, A., Wagner, C., Fialin, M., Gallien, J.P., Wirth, R., Pašava, J., Montagnac, G., 2007. Trace metals and nitrogen in Mo-S-C mixed-layer phases

in Lower Cambrian black shales (Zunyi Formation, Southern China). Chem. Geol. 238, 213–231.
Pašava, J., Kříbek, B., Vymazalová, A., Sýkorová, I., Žák, K., Orberger, B., 2008. Multiple sources of metals of mineralization in lower Cambrian black shales of south china: evidence from geochemical and petrographic study. Resour. Geol. 58, 25–42.
Paytan, A., Mearon, S., Cobb, K., Kastner, M., 2002. Origin of marine barite deposits: Sr and S isotope characterization. Geology 30, 747–750.
Perner, M., Hansen, M., Seifert, R., Strauss, H., Koschinsky, A., Petersen, S., 2013. Linking geology, fluid chemistry, and microbial activity of basalt- and ultramafic-hosted deep-sea hydrothermal vent environments. Geobiology 11, 340–355.
Pi, D.H., Liu, C.Q., Shields-Zhou, G.A., Jiang, S.Y., 2013. Trace and rare earth element geochemistry of black shale and kerogen in the early Cambrian Niutitang Formation in Guizhou province, South China: constraints for redox environments and origin of metal enrichments. Precambrian Res. 225, 218–229.
Qi, L., Hu, J., Gregoire, D.C., 2000. Determination of trace elements in granites by inductively coupled plasma mass spectrometry. Talanta 51, 507–513.
Ravizza, G., Blusztain, J., Von Damm, K.L., Bray, A.M., Bach, W., Hart, S.R., 2001. Sr isotope variations in vent fluids from 9°46′–9°54′N East Pacific Rise: evidence of a non-zero-Mg fluid component. Geochim. Cosmochim. Acta 65, 729–739.
Rudnick, R.L., Gao, S., 2003. Composition of the continental crust. Treatise Geochem. 3, 1–6. http://dx.doi.org/10.1016/B0-08-043751-6/03016-4.
Russell, M.J., Hall, A.J., 1997. The emergence of life from iron monosulphide bubbles at a submarine hydrothermal redox and pH front. J. Geol. Soc. 154, 377–402.
Sawaki, Y., Ohno, T., Fukushi, Y., Komiya, T., Ishikawa, T., Hirata, T., Maruyama, S., 2008. Sr isotope excursion across the Precambrian-Cambrian boundary in the Three Gorges area, South China. Gondwana Res. 14, 134–147.
Schneider, J., Boni, M., Lapponi, F., Bechstädt, T., 2002. Carbonate-hosted zinc-lead deposits in the lower Cambrian of Hunan, South China: a radiogenic (Pb, Sr) isotope study. Econ. Geol. 97, 1815–1827.
Shen, N.P., Peng, J.T., Hu, R.Z., Liu, S., Coulson, T.M., 2010. Strontium and lead isotopic study of the carbonate-hosted Xujiashan antimony deposit from Hubei province, South China: implications for its origin. Resour. Geol. 61, 52–62.
Shi, C.H., Cao, J., Hu, K., Bian, L.Z., Yao, S.P., Zhou, J., Han, S.C., 2014. New understandings of Ni–Mo mineralization in early Cambrian black shales of South China: constraints from variations in organic matter in metallic and non-metallic intervals. Ore Geol. Rev. 59, 73–82.
Shu, D.Y., Hou, B.D., Zhang, M.Q., Xie, X.Y., 2014. Geochemistry and genesis of vanadium deposits in northeastern Guizhou. Mineral Deposits 33, 857–869 (in Chinese with English abstract).
Steiner, M., Wallis, E., Erdtmann, B.D., Zhao, Y.L., Yang, R.D., 2001. Submarine hydrothermal exhalative ore layers in black shales from South China and associated fossils-insights into a Lower Cambrian facies and bio-evolution. Palaeogeogr. Palaeoclimatol. Palaeoecol. 169, 165–191.
Wang, Z.C., Chu, X.L., 1993. Strontium isotopic composition of the early Cambrian barite and witherite deposits. Chin. Sci. Bull. 39, 52–55.
Wang, Z.C., Li, G.Z., 1991. Barite and witherite deposits in Lower Cambrian shales of South China: stratigraphic distribution and geochemical characterization. Econ. Geol. 86, 354–363.
Wang, J.G., Chen, D.Z., Wang, D., Yan, D.T., Zhou, X.Q., Wang, Q.C., 2012. Petrology and geochemistry of chert on the marginal zone of Yangtze Platform, western Hunan, South China, during the Ediacaran-Cambrian transition. Sedimentology 59, 809–829.
Wang, D., Struck, U., Ling, H.F., Guo, Q.J., Shields-Zhou, G.A., Zhu, M.Y., Yao, S.P., 2015a. Marine redox variations and nitrogen cycle of the early Cambrian southern margin of the Yangtze Platform, South China: evidence from nitrogen and organic carbon isotopes. Precambrian Res. 267, 209–226.
Wang, Z.J., Wang, J., Jiang, X.S., Sun, H.Q., Gao, T.S., Chen, J.S., Qiu, Y.S., Du, Q.D., Deng, Q., Yang, F., 2015b. New progress for the stratigraphic division and correlation of Neoproterozoic in Yangtze block, South China. Geol. Rev. 61, 1–22 (in Chinese with English abstract).
Wen, H.J., Carignan, J., 2011. Selenium isotopes trace the source and redox processes in the black shale-hosted Se-rich deposits in China. Geochim. Cosmochim. Acta 75, 1411–1427.
Wen, H.J., Fan, H.F., Zhang, Y.X., Cloquet, C., 2015. Reconstruction of early Cambrian ocean chemistry from Mo isotopes. Geochim. Cosmochim. Acta 164, 1–16.
Xia, F., Ma, D.S., Pan, J.Y., Sun, Z.X., Cao, S.L., Nie, W.M., Wu, K., 2004. Strontium isotopic signature of hydrothermal sedimentation from Early Cambrian barite deposits in east Guizhou, China. Chin. Sci. Bull. 49, 2632–2636.
Xu, L.G., Lehmann, B., Mao, J.W., Nägler, T.F., Neubert, N., Böttcher, M.E., Escher, P., 2012a. Mo isotope and trace element patterns of Lower Cambrian black shales in South China: multi-proxy constraints on the paleoenvironment. Chem. Geol. 318–319, 45–59.
Xu, L.G., Lehmann, B., Mao, J.W., 2012b. Seawater contribution to polymetallic Ni–Mo–PGE–Au mineralization in Early Cambrian black shales of South China: evidence from Mo isotope, PGE, trace element, and REE geochemistry. Ore Geol. Rev. 52, 66–84.
Xu, L.G., Lehmann, B., Zhang, X.G., Zheng, W., Meng, Q.T., 2014. Trace element distribution in black shales from the Kunyang phosphorite deposit and its geological significances. Acta Petrol. Sinica 30, 1817–1827.
Yang, R.D., Wei, H.R., Bao, M., Wang, L., Wang, Q., Zhang, X.D., Liu, L., 2008. Discovery of hydrothermal venting community at the base of Cambrian barite in Guizhou Province, Western China: implication for the Cambrian biological explosion. Prog. Nat. Sci. 18, 65–70.
Žák, K., Pašava, J., Vymazalová, A., Kříbek, B., Chaoyang, L., Deng, H., Mingguo, Z., 2003. Ni-Mo-PGE rich black shales of South China: preliminary results from the isotope study of related barite and carbonates. In: Society for Geology Applied to Mineral Deposits; Mineral Exploration and Sustainable Development. Millpress, Rotterdam, Netherlands, pp. 861–866.
Zeng, M.G., 1998. Geological feature of the Huangjiawan Ni-Mo deposit in Zunyi of Guizhou and its prospect for development. Guizhou Geol. 15, 305–310 (in Chinese with English abstract).
Zhang, J.P., Fan, T.L., Algeo, T.J., Li, Y.F., Zhang, J.C., 2016. Paleo-marine environments of the early Cambrian Yangtze Platform. Palaeogeogr. Palaeoclimatol. Palaeoecol. 443, 66–79.
Zhao, X.F., Zhou, M.F., Gao, J.F., 2015. In situ Sr isotope analysis of apatite by LA-MC-ICPMS: constraints on the evolution of ore fluids of the Yinachang Fe-Cu-REE deposit, Southwest China. Miner. Deposita 50, 871–884.
Zhou, C.M., Jiang, S.Y., 2009. Palaeoceanographic redox environments for the lower Cambrian Hetang Formation in South China: evidence from pyrite framboids, redox sensitive trace elements, and sponge biota occurrence. Palaeogeogr. Palaeoclimatol. Palaeoecol. 271, 279–286.
Zhou, M.Z., Luo, T.Y., Li, Z.X., Zhao, H., Long, H.S., Yang, Y., 2008. SHRIMP U-Pb zircon age of tuff at the bottom of the Lower Cambrian Niutitang Formation, Zunyi, South China. Chin. Sci. Bull. 53, 576–583.
Zhou, J.X., Bai, J.H., Huang, Z.L., Zhu, D., Yan, Z.F., Lv, Z.C., 2015a. Geology, isotope geochemistry and geochronology of the Jinshachang carbonate-hosted Pb–Zn deposit, southwest China. J. Asian Earth Sci. 98, 272–284.
Zhou, X.Q., Chen, D.Z., Dong, S.F., Zhang, Y.Q., Guo, Z.H., Wei, H.W., Yu, H., 2015b. Diagenetic barite deposits in the Yurtus Formation in Tarim Basin, NW China: implications for barium and sulfur cycling in the earliest Cambrian. Precambr. Res. 263, 79–87.
Zhu, B., Jiang, S.Y., Yang, J.H., Pi, D.H., Ling, H.F., Chen, Y.Q., 2014. Rare earth element and Sr-Nd isotope geochemistry of phosphate nodules from the lower Cambrian Niutitang Formation, NW Hunan Province, South China. Palaeogeogr. Palaeoclimatol. Palaeoecol. 398, 132–143.
Zierenberg, R.A., Fouquet, Y., Miller, D.J., 1998. The deep structure of a sea-floor hydrothermal deposit. Nature 392, 485–488.
Zierenberg, R.A., Adams, M.W.W., Arp, A.J., 2000. Life in extreme environments: hydrothermal vents. Proc. Natl. Acad. Sci. U.S.A. 97, 12961–12962.